Magnetic Resonance Imaging 57 (2019) 111–117

Contents lists available at ScienceDirect

Magnetic Resonance Imaging

journal homepage: www.elsevier.com/locate/mri

Original contribution

# Gadoxetic acid-enhanced dynamic magnetic resonance imaging using optimized integrated combination of compressed sensing and parallel imaging technique

Nobuyuki Kawai[a], Satoshi Goshima[a,*], Yoshifumi Noda[a], Kimihiro Kajita[b], Hiroshi Kawada[a], Yukichi Tanahashi[a], Shoma Nagata[a], Masayuki Matsuo[a]

[a] Department of Radiology, Gifu University, 1-1 Yanagido, Gifu 501-1194, Japan
[b] Department of Radiology Services, Gifu University Hospital, 1-1 Yanagido, Gifu 501-1194, Japan

ABSTRACT

*Purpose:* To evaluate the feasibility of optimized integrated combination of compressed sensing and parallel imaging technique (prototype Compressed SENSE) in gadoxetic acid-enhanced dynamic magnetic resonance (MR) imaging.
*Materials and methods:* Sixty-one patients underwent gadoxetic acid-enhanced dynamic imaging using enhanced T1 high-resolution isotropic volume excitation (eTHRIVE) with the Compressed SENSE (CS-eTHRIVE; C SENSE factor, 3.4; acquisition time, 10 s). Results were compared with 61 propensity score-matched patients who underwent conventional eTHRIVE (eTHRIVE; acquisition time, 20 s). For quantitative image analyses, signal intensity ratio (SIR) and signal-to-noise ratio (SNR), coefficient of variation (CV) of liver parenchyma were calculated in each dynamic phase. For qualitative image analyses, two radiologists rated the homogeneity of liver parenchyma, sharpness of liver edge and left external lobe, motion artifacts, and overall image quality in each dynamic phase using a five-point scale.
*Results:* SIRs of liver parenchyma with CS-eTHRIVE were significantly higher than with eTHRIVE in the hepatic arterial phase (HAP) (1.70 vs. 1.52) and transitional phase (TP) (2.18 vs. 2.06) ($P \leq 0.030$). SNR of liver parenchyma were comparable between the two sequences in all phases. CV of liver parenchyma in HAP with eTHRIVE (0.079) was significantly higher than with CS-eTHRIVE (0.065) ($P < 0.001$). Motion artifacts were significantly reduced with CS-eTHRIVE compared with eTHRIVE in all phases ($P \leq 0.005$). The appearance ratio of extensive motion artifacts in HAP with CS-eTHRIVE (0/61; 0%) were significantly reduced compared with eTHRIVE (4/61; 6.6%) ($P = 0.042$). Overall image quality with CS-eTHRIVE was significantly better than with eTHRIVE in all phases ($P \leq 0.039$).
*Conclusion:* CS-eTHRIVE compared with eTHRIVE effectively reduced the acquisition time and extensive motion artifacts without degradation of image quality.

## 1. Introduction

Over the 10 years since gadoxetic acid-enhanced magnetic resonance (MR) imaging was first introduced in daily clinical practice, it has become an essential modality for the screening and assessment of hepatic diseases and is recommended in several clinical guidelines [1,2]. Gadoxetic acid-enhanced dynamic imaging is commonly performed with a sequence of single held breaths of approximately 20 s each using fat-suppressed three-dimensional gradient echo T1-weighted imaging (e.g., enhanced T1 high-resolution isotropic volume excitation or eTHRIVE) after contrast administration [3]. While current accelerated parallel imaging (PI) techniques, for instance, SENSE (sensitivity encoding) [4], can avoid respiratory motion artifacts by reducing acquisition time, patients with compromised breath-holding capacity, such as young children or critically ill adults, often cannot comply with breathing commands, leading to non-dynamic or even non-diagnostic studies. In addition, recent reports suggest that the administration of gadoxetic acid reduces breath-holding capacity in hepatic arterial phase (HAP) and causes transient severe motion (TSM) artifacts [5–10].

Lustig et al. first reported the application of compressed sensing technique for MR imaging in 2007 [11], subsequently, MR imaging with Cartesian trajectories was more accelerated using the combination of compressed sensing and PI technique [12]. The compressed sensing technique has recently been developed by advances in graphic data processing and applied in clinical settings [13–16]. In this study, we assessed eTHRIVE sequence using optimized integrated combination of compressed sensing and PI technique (prototype Compressed SENSE) for liver dynamic imaging. It was hypothesized that the reduction of acquisition time for dynamic liver MR imaging could significantly reduce the motion artifacts and contribute to better image quality. The purpose of this study was to evaluate the feasibility of the Compressed SENSE technique in gadoxetic acid-enhanced dynamic MR imaging.

* Corresponding author.
*E-mail address:* gossy@par.odn.ne.jp (S. Goshima).

https://doi.org/10.1016/j.mri.2018.11.004
Received 3 September 2018; Received in revised form 26 October 2018; Accepted 11 November 2018

## 2. Materials and methods

### 2.1. Patients

This prospective HIPAA-compliant study was approved by our institutional review board. Written informed consent was obtained from all patients. The study population was composed of consecutive patients between January and August 2017 who received gadoxetic acid-enhanced MR imaging using a 3-Tesla (T) clinical scanner with a 32-channel phased-array receiver coil (Ingenia CX; Philips Healthcare, Best, The Netherlands). Before the introduction of the Compressed SENSE technique, 146 patients underwent gadoxetic acid-enhanced conventional eTHRIVE (eTHRIVE) between January and April 2017. Gadoxetic acid-enhanced eTHRIVE with the Compressed SENSE (CS-eTHRIVE) was obtained in 70 patients after its introduction in May 2017. Five patients who underwent eTHRIVE were excluded because of technical failure. Accordingly, 211 patients were included in this study cohort. Patients who had CS-eTHRIVE were propensity score-matched with patients who had eTHRIVE based on age, gender, body mass index, Child-Pugh Score for Cirrhosis Mortality, and presence or absence of pulmonary emphysema, interstitial pneumonia, and pleural effusion. Eighty-nine patients who lacked a matched control were excluded. A cumulative total of 122 patients constituted the final study population including 61 who had CS-eTHRIVE (43 men and 18 women; mean age, 67.9 ± 11.7 years; age range, 27–84 years) and 61 who had eTHRIVE (46 men and 15 women; mean age, 67.6 ± 14.1 years; age range, 33–89 years). Demographics of the final study population are summarized in Fig. 1 and Table 1.

**Table 1**
Demographics of study population.

| Variables | |
|---|---|
| Sex, M:F | 89:33 |
| Age (years) | 67.7 ± 12.9 (27–89) |
| BMI (kg/m$^2$) | 23.0 ± 3.3 (15.2–32.0) |
| Underlying liver disease | |
| Chronic hepatitis B | 22.1% (27/122) |
| Chronic hepatitis C | 27.0% (33/122) |
| Non-B Non-C | 3.3% (4/122) |
| NASH | 3.3% (4/122) |
| Healthy liver | 45.9% (56/122) |
| Child-Pugh score, 5/6/7/8 | 81.1% (99/122)/16.3% (20/122)/0.8% (1/122)/1.6% (2/122) |
| Laboratory findings | |
| Albumin (g/dL) | 4.1 ± 0.4 (2.6–5.1) |
| Total bilirubin (mg/dL) | 0.9 ± 0.4 (0.3–2.2) |
| Prothrombin time (%) | 98.3 ± 14.3 (63–120) |
| Ascites, yes | 5.7% (7/122) |
| Pulmonary emphysema, yes | 13.9% (17/122) |
| IP, yes | 2.5% (3/122) |
| Pleural effusion, yes | 4.1% (5/122) |

Note. –Data are means ± 1 standard deviation. Numbers in parentheses are ranges or ratio. BMI = body mass index. NASH = non-alcoholic steatohepatitis. IP = interstitial pneumonia.

### 2.2. Routine MR image acquisition technique

The routine MR imaging protocol included the following sequences: 1) breath-holding two-dimensional dual-echo axial T1-weighted fast field-echo imaging [repetition time (TR)/echo time (TE), 216/2.35 ms in-phase and 216/1.15 ms opposed-phase]; 2) respiratory-triggered two-dimensional fat-suppressed axial T2-weighted turbo spin-echo imaging (TR/TEeff, 1800/80 ms); 3) free-breathing diffusion-weighted echo-planar imaging (TR/TE, 5000/63 ms); and 4) breath-holding gadoxetic acid-enhanced dynamic and hepatobiliary phase imaging with a fat-suppressed three-dimensional spoiled axial fast field-echo sequence (CS-eTHRIVE or eTHRIVE). Scan parameters in CS-eTHRIVE and eTHRIVE sequences are summarized in Table 2.

After obtaining precontrast-enhanced phase (PCP) images, 0.025 mmol/kg body weight (0.1 mL/kg) of gadoxetic acid (Eovist or Primovist; Bayer AG, Leverkusen, Germany) were administered with 30 mL saline flush at a rate of 1 mL/s. Subsequently, contrast-enhanced dynamic images were obtained in HAP, portal venous phase (PVP), and transitional phase (TP) at 5, 45, and 115 s, respectively, after the peak

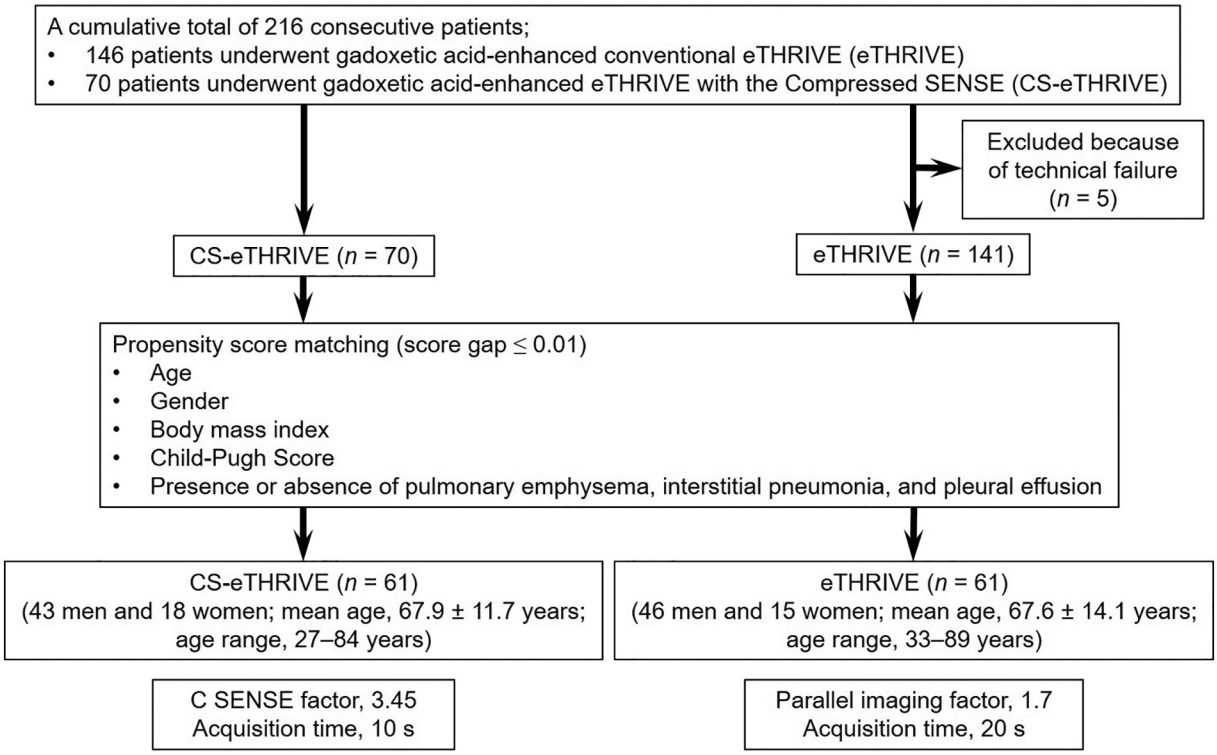


**Fig. 1.** Flow diagram for patient selection in this study cohort.

**Table 2**
Scan parameters in CS-eTHRIVE and eTHRIVE sequences.

| Parameter | CS-eTHRIVE | eTHRIVE |
|---|---|---|
| Respiratory control | Breath hold | Breath hold |
| Sequence | 3D fast field echo | 3D fast field echo |
| Fat suppression | Yes | Yes |
| Repetition time (TR)/echo time (TE) (msec) | 3.3/1.56 | 3.3/1.56 |
| Flip angle (degree) | 15 | 15 |
| Field of view (cm) | 42 × 29.4 | 42 × 29.4 |
| Matrix | 304 × 249 (512 recon) | 304 × 249 (512 recon) |
| SENSE factor | – | 1.7 |
| C SENSE factor | 3.45 | – |
| Slice thickness (mm) | 4 | 4 |
| Intersection gap (mm) | −2 | −2 |
| No. of sections | 90 | 90 |
| Acquisition time (sec) | 10 | 20 |

aortic contrast enhancement detected by fluoroscopic bolus tracking system. All injections were performed using a commercially available power injector (Blinded).

### 2.3. Compressed SENSE

The reconstruction of the images was based on the prototype Compressed SENSE algorithm provided by Philips (Philips Healthcare, Best, The Netherlands). Lustig et al. [11] introduced compressed sensing techniques used for under-sampling and reconstruction. In our study, we use the Compressed SENSE algorithm which is based on the combination of compressed sensing and SENSE PI, using a variable density incoherent under-sampling acquisition and an integrated iterative reconstruction loop. The Compressed SENSE scheme optimizes both the acquisition and the reconstruction. The under-sampling scheme acquires the k-space data with a smoothly varying density, decreasing from the center of k-space to the periphery. The reconstruction was based on minimizing the function:

$$\left(\sum_{i=1}^{\#coils} \|m_i - ES_i p\|_2^2 + \lambda_1 \|R^{-1/2} p\|_2^2 + \lambda_2 \|\Psi p\|_1\right)$$

where $m_i$ is the measured data for a given coil element $i$, $E$ is the under-sampling Fourier operator as defined by the sampling pattern, $S_i$ represents the coil sensitivities, $p$ is the image, $R$ constrains the solution to areas where the reference scan shows signal and $\Psi$ is the sparsity transform, here into the wavelet domain. $\lambda 1$ and $\lambda 2$ are regularization factors.

The minimization is implemented in an integrated iterative loop with two kinds of regularization used simultaneously. The regularization factor ($\lambda 1$) balances between data consistency and prior knowledge of image content, and the regularization factor ($\lambda 2$) is used to balance the sparsity constraint and data consistency in the iterative solution.

In the Compressed SENSE reconstruction algorithm, SENSE unwrapping is followed by sparse transformation and denoising (compressed sensing). These SENSE unwrapping and denoising processes are executed iteratively to minimize the above cost function. The Compressed SENSE implementation optimizes both the sampling pattern and the regularization factors fully automatically, for any anatomy, image contrast, acceleration factor or receiver coils used.

### 2.4. Quantitative image analysis

Quantitative measurements were conducted by a radiologist with 7 years of post-training experience in interpreting body MR imaging. The mean signal intensities of the liver parenchyma ($SI_{Liver}$) and the paraspinal muscle ($SI_{muscle}$), and the standard deviation of the liver parenchyma ($SD_{Liver}$) and the paraspinal muscle ($SD_{muscle}$) in each dynamic phase were measured by placing a circular region of interest (ROI) cursor ranging from 20 to 30 mm in diameter. ROI measurements of the liver parenchyma were conducted on the right anterior, right posterior, left internal, and left external segments, avoiding intrahepatic blood vessels. The signal intensity ratio (SIR), signal-to-noise ratio (SNR), and coefficient of variation (CV) of 4 liver segments were calculated as $SI_{Liver}/SI_{muscle}$, $SI_{Liver}/SD_{muscle}$, and $SD_{Liver}/SI_{Liver}$, and then averaged, respectively.

### 2.5. Qualitative image analysis

Image quality was independently evaluated by two radiologists (with 17 and 8 years of post-training experience in interpreting body MR imaging). Qualitative ratings in each dynamic phase were recorded on a 5-point scale (1 = unacceptable, 2 = suboptimal, 3 = acceptable, 4 = good, and 5 = excellent), evaluating homogeneity of liver parenchyma, sharpness of liver edge and left external lobe, and overall image quality. Additionally, the radiologists assigned the following motion artifact scores in each dynamic phase using prior studies as a reference [5, 6]: 1 = extensive motion artifacts with non-diagnostic images, 2 = severe motion artifacts with images degraded but interpretable, 3 = moderate motion artifacts with some but not severe effects on diagnostic quality, 4 = minimal motion artifacts with no effect on diagnostic quality, and 5 = no motion artifacts. Finally, the radiologists recorded consensus scores on qualitative and motion artifact scores. TSM artifacts were defined as the following combination of motion artifact scores: ≥4 in PCP, ≤2 in HAP, and ≥4 in PVP and/or TP [5,6].

### 2.6. Statistical analysis

Statistical analyses were performed using commercially available software (IBM SPSS Statistics for Windows, version 24.0; IBM Corp., Armonk, NY, USA). Propensity score matching was performed to match the two groups, and score gap was set to 0.01 or less. Unpaired *t*-test was used to evaluate differences in SIR, SNR, and CV between the two-sequence groups. Qualitative scores and motion artifact score between the two-sequence groups were compared using Mann–Whitney *U* test. Chi-square test or Fisher's exact test was performed to compare the appearance ratio of TSM artifacts or extensive motion artifacts (motion artifact score = 1) between the two-sequence groups. A *P* value of $< 0.05$ was considered statistically significant.

For a qualitative assessment of interobserver variability, weighted kappa statistics were used to measure the degree of agreement. A kappa value of up to 0.20 was interpreted as slight agreement, 0.21–0.40 was fair agreement, 0.41–0.60 was moderate agreement, 0.61–0.80 was substantial agreement, and 0.81 or greater was almost perfect agreement.

## 3. Results

### 3.1. Quantitative image analysis

Table 3 shows the quantitative measurements in CS-eTHRIVE and eTHRIVE sequences. SIRs of liver parenchyma with CS-eTHRIVE were significantly higher than with eTHRIVE in HAP (1.70 vs. 1.52) and TP (2.18 vs. 2.06) ($P \leq 0.030$). SNRs of liver parenchyma were comparable between the two sequences in all phases. CV of liver parenchyma in HAP with eTHRIVE (0.079) was significantly higher than with CS-eTHRIVE (0.065) ($P < 0.001$). No significant difference was found between the two sequences in other measurements.

### 3.2. Qualitative image analysis

Table 4 shows the qualitative scores in CS-eTHRIVE and eTHRIVE sequences. Homogeneity of liver parenchyma in HAP with CS-eTHRIVE (3.64) was significantly better than with eTHRIVE (3.44) ($P = 0.003$).

**Table 3**
Quantitative measurements in CS-eTHRIVE and eTHRIVE sequences.

| Parameter | Phase | CS-eTHRIVE | eTHRIVE | *P* value |
|---|---|---|---|---|
| SIR | PCP | 1.55 ± 0.25 | 1.56 ± 0.54 | 0.937 |
| | HAP | 1.70 ± 0.34 | 1.52 ± 0.25 | 0.002 |
| | PVP | 2.31 ± 0.75 | 2.10 ± 0.40 | 0.057 |
| | TP | 2.18 ± 0.32 | 2.06 ± 0.28 | 0.030 |
| SNR | PCP | 28.0 ± 9.8 | 29.4 ± 15.0 | 0.566 |
| | HAP | 27.6 ± 11.1 | 26.4 ± 11.6 | 0.565 |
| | PVP | 39.3 ± 14.5 | 41.3 ± 16.2 | 0.467 |
| | TP | 38.9 ± 13.2 | 40.9 ± 14.9 | 0.438 |
| CV | PCP | 0.060 ± 0.009 | 0.059 ± 0.013 | 0.546 |
| | HAP | 0.065 ± 0.016 | 0.079 ± 0.019 | < 0.001 |
| | PVP | 0.045 ± 0.010 | 0.044 ± 0.010 | 0.572 |
| | TP | 0.040 ± 0.009 | 0.039 ± 0.009 | 0.773 |

Note. –Data are means ± 1 standard deviation. SIR = signal intensity ratio. SNR = signal-to-noise ratio. CV = coefficient of variation. PCP = precontrast-enhanced phase. HAP = hepatic arterial phase. PVP = portal venous phase. TP = transitional phase.

Motion artifacts were significantly reduced with CS-eTHRIVE compared with eTHRIVE in all phases ($P \leq 0.005$). The appearance ratio of TSM artifacts was improved with CS-eTHRIVE (6/61; 9.8%) compared with eTHRIVE (11/61; 18.0%) ($P = 0.191$). The appearance ratio of extensive motion artifacts (motion artifact score = 1) in HAP were significantly reduced with CS-eTHRIVE (0/61; 0%) compared with eTHRIVE (4/61; 6.6%) ($P = 0.042$) (Fig. 2).

Overall image quality with CS-eTHRIVE was significantly higher than with eTHRIVE in all phases ($P \leq 0.039$) (Figs. 3–4). The kappa values of independent ratings for qualitative scores by two observers ranged from 0.701 to 0.879, indicating substantial to almost perfect agreement.

## 4. Discussion

The very nature of the compressed sensing technique offers a significant reduction of acquisition time by recovering image information from highly under-sampled k-space data [11]. In general, under-sampled k-space data results in the severe degradation of signal intensity and image quality. Although we attempted 50% reduction in acquisition time using CS-eTHRIVE, our quantitative result demonstrated that SIRs of liver parenchyma with CS-eTHRIVE are equivalent to those with eTHRIVE. We believed that this is because the optimized under-sampling pattern and the regularization factors by the Compressed SENSE make up for the degradation of signal intensity and image quality. Furthermore, SNRs of liver parenchyma with CS-eTHRIVE were also equivalent to those with eTHRIVE. These results mean that the Compressed SENSE denoising algorithm effectively decreases the image noise. Additionally, motion artifacts cause the homogeneity of $SI_{Liver}$ to fluctuate, resulting in increased $SD_{Liver}$. As motion artifacts in HAP with eTHRIVE (which are the most severe of all dynamic phases) increase $SD_{Liver}$, CV of liver parenchyma in HAP with eTHRIVE is significantly higher than with CS-eTHRIVE. Generally, CV showed signal variation within the ROI. Therefore, our results indicated that CS-eTHRIVE could provide more homogeneous image in HAP compared with eTHRIVE.

Gadoxetic acid is liver-specific contrast agent that is useful for hemodynamic analyses of liver diseases and to visualize whether there is functional hepatocyte in the hepatobiliary phase [17]. However, dynamic imaging, especially in HAP, is still challenging for patients with limited breath-holding capabilities. Our results demonstrate that CS-eTHRIVE reduces the breath-holding acquisition time by one-half compared with conventional eTHRIVE (10 vs. 20 s), resulting in less motion artifacts in all phases, especially in HAP. In fact, TSM artifacts in CS-eTHRIVE (9.8%) were reduced compared with eTHRIVE (18.0%). Most notably, extensive motion artifacts (motion artifact score = 1) in HAP with CS-eTHRIVE (0%) were significantly reduced compared with conventional eTHRIVE (6.6%). TSM artifacts with conventional eTHRIVE were comparable to those in previously reported data (6.8%–18.3%) [5–7,10]. TSM artifacts are unpreventable when gadoxetic acid is used; however, CS-eTHRIVE can avoid non-diagnostic study results caused by extensive motion artifacts.

**Table 4**
Qualitative scores in CS-eTHRIVE and eTHRIVE sequences.

| Parameter | Sequence | | *P* value |
|---|---|---|---|
| | CS-eTHRIVE | eTHRIVE | |
| Homogeneity of liver parenchyma | | | |
| PCP | 3.57 ± 0.64 (2–5) | 3.48 ± 0.71 (2–5) | 0.131 |
| HAP | 3.64 ± 0.63 (3–5) | 3.44 ± 0.74 (2–5) | 0.003 |
| PVP | 3.95 ± 0.62 (3–5) | 3.88 ± 0.68 (2–5) | 0.229 |
| TP | 4.00 ± 0.61 (3–5) | 3.93 ± 0.68 (2–5) | 0.350 |
| Sharpness of liver edge | | | |
| PCP | 3.34 ± 0.54 (2–5) | 3.39 ± 0.60 (2–5) | 0.387 |
| HAP | 3.54 ± 0.65 (2–5) | 3.45 ± 0.77 (1–5) | 0.186 |
| PVP | 4.26 ± 0.48 (3–5) | 4.18 ± 0.60 (3–5) | 0.211 |
| TP | 4.49 ± 0.54 (3–5) | 4.39 ± 0.57 (3–5) | 0.067 |
| Sharpness of left external lobe | | | |
| PCP | 3.51 ± 0.57 (3–5) | 3.51 ± 0.58 (3–5) | 0.930 |
| HAP | 3.30 ± 0.72 (2–5) | 3.28 ± 0.79 (1–5) | 0.967 |
| PVP | 3.92 ± 0.67 (3–5) | 3.83 ± 0.68 (2–5) | 0.158 |
| TP | 4.07 ± 0.63 (3–5) | 3.96 ± 0.65 (3–5) | 0.068 |
| Motion artifact | | | |
| PCP | 4.10 ± 0.70 (2–5) | 3.70 ± 0.80 (2–5) | 0.005 |
| HAP | 3.62 ± 1.05 (2–5) | 2.93 ± 1.01 (1–5) | 0.001 |
| PVP | 4.41 ± 0.62 (3–5) | 3.87 ± 0.90 (2–5) | 0.001 |
| TP | 4.44 ± 0.59 (3–5) | 4.03 ± 0.77 (2–5) | 0.002 |
| Overall image quality | | | |
| PCP | 3.67 ± 0.65 (2–5) | 3.53 ± 0.72 (2–5) | 0.017 |
| HAP | 3.38 ± 0.92 (2–5) | 3.07 ± 1.01 (1–5) | 0.001 |
| PVP | 4.21 ± 0.52 (3–5) | 4.02 ± 0.75 (2–5) | 0.012 |
| TP | 4.26 ± 0.55 (3–5) | 4.12 ± 0.66 (2–5) | 0.039 |

Note. –Data are means ± 1 standard deviation. Numbers in parentheses are ranges. PCP = precontrast-enhanced phase. HAP = hepatic arterial phase. PVP = portal venous phase. TP = transitional phase.

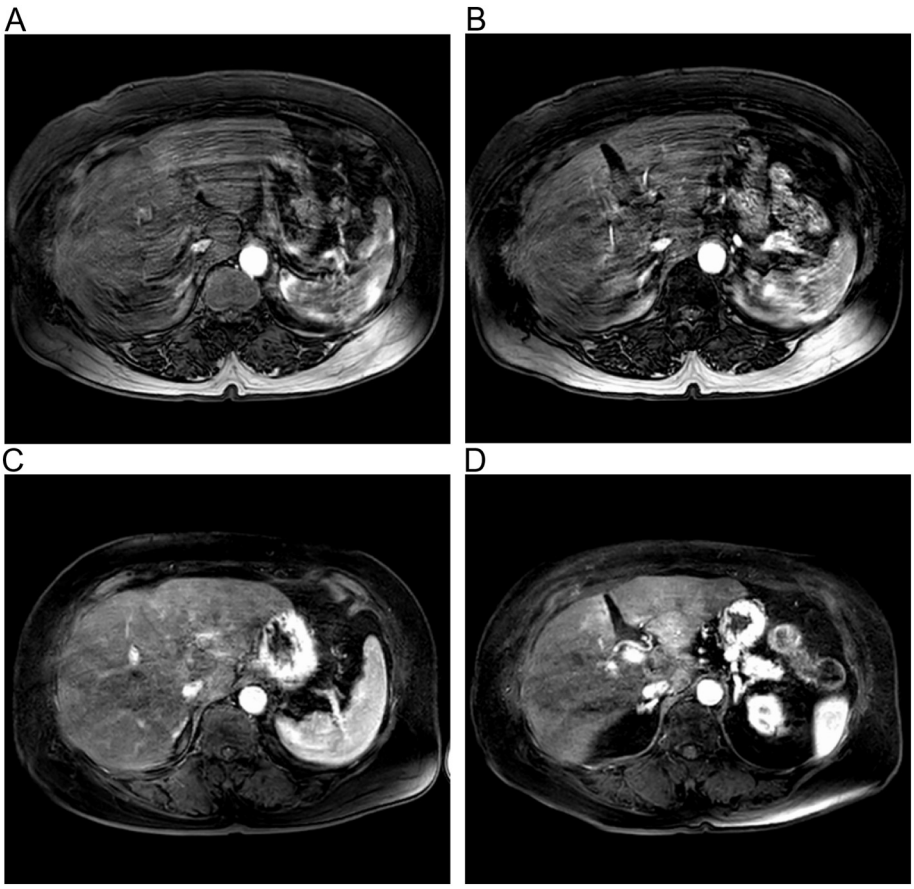


**Fig. 2.** A 73-year-old female status post partial hepatectomy for hepatocellular carcinoma without viral hepatitis, who underwent gadoxetic acid-enhanced dynamic MR imaging with both eTHRIVE and CS-eTHRIVE technique at different times in the study period. Extensive motion artifacts were observed in hepatic arterial phase images (A, maximum parting plane; B, hepatic hilar level) with eTHRIVE (overall image quality scores of 1), whereas only mild artifacts were observed in those (C, maximum parting plane; D, hepatic hilar level) with CS-eTHRIVE (overall image quality scores of 3).

The multiple arterial phase acquisition technique [18] is one of the solutions to eliminate TSM artifacts. Pietryga et al. [7] reported that the use of this technique provided at least one adequate arterial phase in most of patients with TSM artifacts (81%). This technique enables low temporal resolution (e.g., 7.5 s per phase [7]), however, it sacrifices SNR using partial Fourier under-sampling and z-axial spatial resolution compared with our study (slice thickness/intersection gap; 4/0 vs. 4/−2). On the other hand, the free-breathing technique or the radial k-

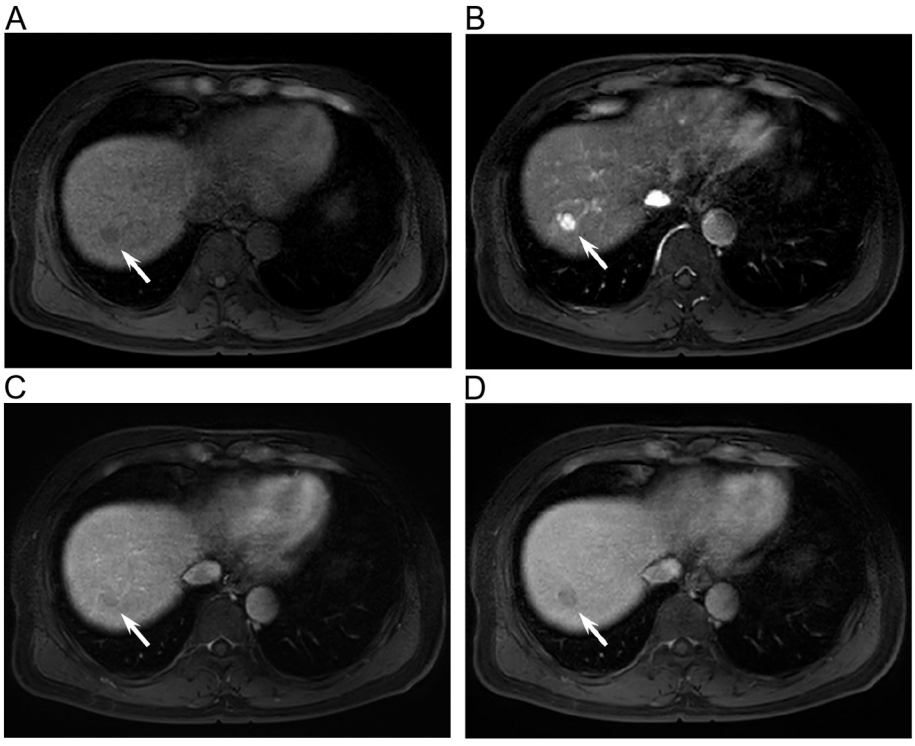


**Fig. 3.** A 55-year-old male with chronic hepatitis C post direct-acting antiviral therapy. Gadoxetic acid-enhanced dynamic MR imaging with CS-eTHRIVE (A, pre-contrast; B, hepatic arterial phase; C, portal venous phase; D, transitional phase) demonstrated excellent image quality without motion artifacts (overall image quality score of 5). A hypervascular hepatocellular nodule was noted in segment VII (arrow).

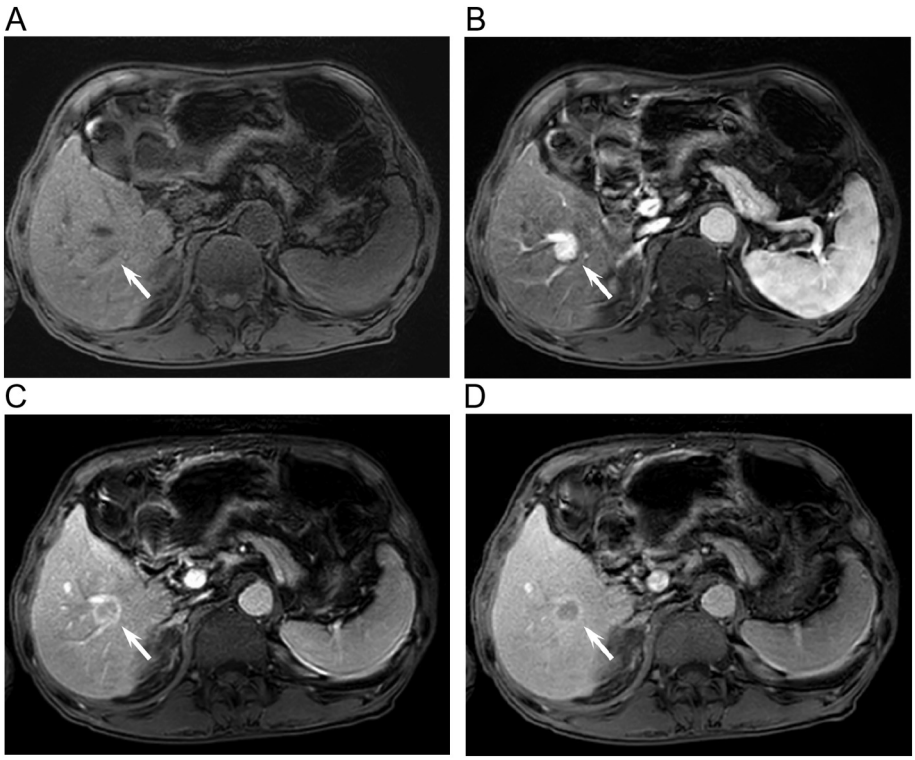


**Fig. 4.** A 66-year-old male with chronic hepatitis B. Gadoxetic acid-enhanced dynamic MR imaging with eTHRIVE (A, pre-contrast; B, hepatic arterial phase; C, portal venous phase; D, transitional phase) demonstrated acceptable image quality with moderate motion artifacts (overall image quality scores of 3 for A and B, and 4 for C and D).

space sampling technique [19,20] is also another solution to eliminate TSM artifacts. Although it has been widely used for dynamic liver imaging in patients with limited breath-holding capability, the degradation of spatial resolution in the plane compared with the Cartesian sampling is the greatest disadvantage [21,22]. Therefore, it is difficult for the radial k-space sampling technique to achieve as same spatial resolution as the Cartesian sampling, especially during a hepatic artery dominant phase.

This study has some limitations. First, study population was relatively small with single center study. Second, we did not evaluate the diagnostic performance of focal hepatic lesions, however, we believe that CS-eTHRIVE sequence have the potential to yield better conspicuity of focal hepatic lesions due to less motion artifacts and better overall image quality. Further clinical studies should be performed in a larger population to validate our results.

In conclusion, CS-eTHRIVE effectively reduces the acquisition time, contributing to a significant reduction of motion artifact and improvement of overall image quality for gadoxetic acid-enhanced dynamic MR imaging.

## Conflicts of interest

We have no known conflicts of interest associated with this publication and there has been no financial support for this work that could have influenced its outcome.

## References

[1] Kudo M, Matsui O, Izumi N, Iijima H, Kadoya M, Imai Y. Surveillance and diagnostic algorithm for hepatocellular carcinoma proposed by the Liver Cancer Study Group of Japan: 2014 update. Oncology 2014;87(Suppl. 1):7–21.
[2] Omata M, Cheng AL, Kokudo N, Kudo M, Lee JM, Jia J, et al. Asia-Pacific clinical practice guidelines on the management of hepatocellular carcinoma: a 2017 update. Hepatol Int 2017;11(4):317–70.
[3] Goshima S, Noda Y, Kajita K, Kawai N, Koyasu H, Kawada H, et al. Gadoxetic acid-enhanced high temporal-resolution hepatic arterial-phase imaging with view-sharing technique: impact on the LI-RADS category. Eur J Radiol 2017;94:167–73.
[4] Pruessmann KP, Weiger M, Scheidegger MB, Boesiger P. SENSE: sensitivity encoding for fast MRI. Magn Reson Med 1999;42(5):952–62.
[5] Davenport MS, Viglianti BL, Al-Hawary MM, Caoili EM, Kaza RK, Liu PS, et al. Comparison of acute transient dyspnea after intravenous administration of gadoxetate disodium and gadobenate dimeglumine: effect on arterial phase image quality. Radiology 2013;266(2):452–61.
[6] Davenport MS, Caoili EM, Kaza RK, Hussain HK. Matched within-patient cohort study of transient arterial phase respiratory motion-related artifact in MR imaging of the liver: gadoxetate disodium versus gadobenate dimeglumine. Radiology 2014;272(1):123–31.
[7] Pietryga JA, Burke LM, Marin D, Jaffe TA, Bashir MR. Respiratory motion artifact affecting hepatic arterial phase imaging with gadoxetate disodium: examination recovery with a multiple arterial phase acquisition. Radiology 2014;271(2):426–34.
[8] Bashir MR, Castelli P, Davenport MS, Larson D, Marin D, Hussain HK, et al. Respiratory motion artifact affecting hepatic arterial phase MR imaging with gadoxetate disodium is more common in patients with a prior episode of arterial phase motion associated with gadoxetate disodium. Radiology 2015;274(1):141–8.
[9] Motosugi U, Bannas P, Bookwalter CA, Sano K, Reeder SB. An investigation of transient severe motion related to gadoxetic acid-enhanced MR imaging. Radiology 2016;279(1):93–102.
[10] McClellan TR, Motosugi U, Middleton MS, Allen BC, Jaffe TA, Miller CM, et al. Intravenous gadoxetate disodium administration reduces breath-holding capacity in the hepatic arterial phase: a multi-center randomized placebo-controlled trial. Radiology 2017;282(2):361–8.
[11] Lustig M, Donoho D, Pauly JM. Sparse MRI: the application of compressed sensing for rapid MR imaging. Magn Reson Med 2007;58(6):1182–95.
[12] Liang D, Liu B, Wang J, Ying L. Accelerating SENSE using compressed sensing. Magn Reson Med 2009;62(6):1574–84.
[13] Kaltenbach B, Bucher AM, Wichmann JL, Nickel D, Polkowski C, Hammerstingl R, et al. Dynamic liver magnetic resonance imaging in free-breathing: feasibility of a Cartesian T1-weighted acquisition technique with compressed sensing and additional self-navigation signal for hard-gated and motion-resolved reconstruction. Invest Radiol 2017;52(11):708–14.
[14] Seo N, Park MS, Han K, Kim D, King KF, Choi JY, et al. Feasibility of 3D navigator-triggered magnetic resonance cholangiopancreatography with combined parallel imaging and compressed sensing reconstruction at 3T. J Magn Reson Imaging 2017;46(5):1289–97.
[15] Weiss J, Notohamiprodjo M, Martirosian P, Taron J, Nickel MD, Kolb M, et al. Self-gated 4D-MRI of the liver: Initial clinical results of continuous multiphase imaging of hepatic enhancement. J Magn Reson Imaging 2018;47(2):459–67.
[16] Yoon JH, Yu MH, Chang W, Park JY, Nickel MD, Son Y, et al. Clinical feasibility of free-breathing dynamic T1-weighted imaging with gadoxetic acid-enhanced liver magnetic resonance imaging using a combination of variable density sampling and compressed sensing. Invest Radiol 2017;52(10):596–604.
[17] Sano K, Ichikawa T, Motosugi U, Sou H, Muhi AM, Matsuda M, et al. Imaging study of early hepatocellular carcinoma: usefulness of gadoxetic acid-enhanced MR imaging. Radiology 2011;261(3):834–44.
[18] Bashir MR, Gupta RT, Davenport MS, Allen BC, Jaffe TA, Ho LM, et al. Hepatocellular carcinoma in a North American population: does hepatobiliary MR imaging with Gd-EOB-DTPA improve sensitivity and confidence for diagnosis? J

Magn Reson Imaging 2013;37(2):398–406.
[19] Chandarana H, Feng L, Block TK, Rosenkrantz AB, Lim RP, Babb JS, et al. Free-breathing contrast-enhanced multiphase MRI of the liver using a combination of compressed sensing, parallel imaging, and golden-angle radial sampling. Invest Radiol 2013;48(1):10–6.
[20] Kaltenbach B, Roman A, Polkowski C, Gruber-Rouh T, Bauer RW, Hammerstingl R, et al. Free-breathing dynamic liver examination using a radial 3D T1-weighted gradient echo sequence with moderate undersampling for patients with limited breath-holding capacity. Eur J Radiol 2017;86:26–32.
[21] Chandarana H, Block TK, Rosenkrantz AB, Lim RP, Kim D, Mossa DJ, et al. Free-breathing radial 3D fat-suppressed T1-weighted gradient echo sequence: a viable alternative for contrast-enhanced liver imaging in patients unable to suspend respiration. Invest Radiol 2011;46(10):648–53.
[22] Kajita K, Goshima S, Noda Y, Kawada H, Kawai N, Okuaki T, et al. Thin-slice free-breathing pseudo-golden-angle radial stack-of-stars with gating and tracking T1-weighted acquisition: an efficient gadoxetic acid-enhanced hepatobiliary-phase imaging alternative for patients with unstable breath holding. Magn Reson Med Sci 2018. https://doi.org/10.2463/mrms.mp.2017-0173.